Shahid Chamran University of Ahvaz

Iranian Association of Electrical and Electronics Engineers

**Journal of Applied Research in Electrical Engineering**

E-ISSN: 2783-2864
P-ISSN: 2717-414X
Homepage: http://jaree.scu.ac.ir/

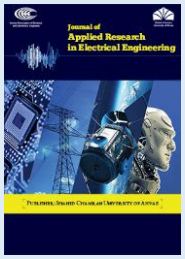

**Research Article**

# Reactive Power Coordination Between Solid Oxide Fuel Cell and Battery for Microgrid Frequency Control

**Saeed Aminzadeh [1,2,*], Mehrdad Tarafdar Hagh [1,3], and Heresh Seyedi [1]**

[1] *Faculty of Electrical and Computer Engineering, University of Tabriz, 29 Bahman Blvd, Tabriz 51666-16471, Iran*
[2] *Engineering Faculty, Islamic Azad University, Ravansar, Kermanshah, Iran*
[3] *Engineering Faculty, Near East University, 99138 Nicosia, North Cyprus, Mersin 10, Turkey*
[*] *Corresponding Author: saeed.aminzadeh1363@gmail.com*

**Abstract: This paper uses the coordination between the reactive power of a solid oxide fuel cell (SOFC) and a battery to control the frequency within an islanded microgrid. By this coordination, the microgrid frequency regulation becomes faster and better during contingencies. Moreover, the energy storage capacity, which is usually required for the frequency control of islanded microgrids, has significantly been reduced. Furthermore, there will be no need to consider reserve capacity in renewable sources for frequency control. Therefore, renewable energy sources can be operated at their maximum power point. Also, this paper introduces a new frequency-reactive power control concept and a related coefficient that shows the degree of dependence of the microgrid frequency on the injected reactive power changes at each bus. This coefficient determines the priority of buses for the installation of reactive power control devices to control the frequency of the microgrid. Simulation studies have been performed in the MATLAB/Simulink environment. The results show the applicability and accuracy of the proposed coefficient and demonstrate the effectiveness of the coordinated control of reactive power between the SOFC and the battery for frequency control.**

**Keywords:** Microgrid frequency control, solid oxide fuel cell (SOFC), coordinated control of reactive power, frequency-reactive power coefficient.

**Article history**
Received 17 April 2021; Revised 13 August 2021; Accepted 13 August 2021; Published online 23 February 2022

**How to cite this article**
S. Aminzadeh, M. T. Hagh, and H. Seyedi, "Reactive power coordination between solid oxide fuel cell and battery for microgrid frequency control," *J. Appl. Res. Electr. Eng.*, vol. 1, no. 2, pp. 121-130, 2022.
DOI:10.22055/jaree.2021.37177.1028

Check for updates

## 1. INTRODUCTION

When a microgrid is connected to the upstream grid, the imbalance between the generated power and the consumed power in the microgrid is compensated by the upstream grid. Consequently, the frequency of the microgrid is always equal to the frequency of the upstream grid. However, in the disconnected state, the microgrid loses its powerful support. As a result, a fast balance between the generated power and the consumed power in the microgrid is essential for frequency control. Previous studies in this field have proposed various solutions for frequency control, such as the application of fast-response energy storage devices like batteries, demand response programs, the concepts of virtual synchronous generator and virtual inertia creation, load shedding in emergency cases, and the operation of renewable and sustainable energy resources at points other than maximum power points. Some relevant works are reviewed below.

References [1-2] investigated the need for energy storage devices and load shedding strategies for the frequency control and the operation of islanded microgrids. Reference [3] studied the influence of the fluctuations in wind and solar radiation on changes in the microgrid frequency. It demonstrated that the fast performance of a battery energy storage system can mitigate this effect on the dynamic operation of the microgrid. A battery energy storage system was proposed in [4-5] to support the frequency control process in a microgrid with high penetration of renewable energy resources. Reference [6] presented a new concept of the primary frequency control by integrating the superconducting magnetic energy storage (SMES) with the battery, which not only allowed performing a good frequency regulating function but also extended the battery service time.

A novel coordinated control scheme using the demand-side management was presented in [7-8] for an islanded microgrid. Reference [9] investigated the impact of load dynamics and load sharing among inverter-interfaced distributed generation units on the frequency stability and the dynamic performance of the islanded ac microgrids. Reference [10] introduced new functions for online execution, which are capable of managing microgrid storage by taking into account the electric vehicles and the load response with the purpose of frequency control. Reference [11] proposed a new load frequency control strategy for microgrids in which electric vehicles are considered. Various centralized and decentralized dynamic load response methods were presented in [12] for controlling the initial frequency in a microgrid. Reference [13] proposed a flexible and effective control scheme for determining the size and location of loads that need shedding in order to maintain frequency within permissible limits. In [14], an auxiliary frequency control loop was added to the synchronous generator excitation system present in a microgrid. Also, an excitation was employed in addition to the governor to control the frequency using the synchronous generators. Reference [15] introduced a hierarchical control structure composed of the primary, secondary, and tertiary controllers to be used in islanded microgrids. Reference [16] presented a multi-level control architecture for the autonomous operation of the islanded microgrids with power electronic interfaces. Virtual inertia control strategies that would contribute to frequency regulation in a microgrid were proposed in [17-20]. Reference [21] presented a novel frequency and voltage control method for islanded microgrids based on a distributed hybrid control. Reference [22] proposed a decentralized control method to stabilize microgrid frequency and voltage and also to distribute generation among the distributed generations. Reference [23] presented a novel control method for the load voltage and system frequency during the islanding of the microgrid for a multi-zone power system composed of several microgrids. A number of control and management strategies were presented in [24] for coordinating microgrid resources to regulate the voltage and frequency in order to operate the microgrid independently and optimally. Reference [25] utilized a novel optimal model-less controller to create a balance between the load demand and the power generation and, as a result, to control the frequency in the islanded microgrid. Reference [26] explored the development of an internal model-based controller approach for better frequency regulation in a hybrid microgrid. In [27], an innovative independent control method was proposed for accurate division of the reactive power among the scattered energy sources and also the frequency recovery of the microgrid. Reference [28] presented a control method for dg's to simultaneously distribute the active power and recover the frequency in an islanded microgrid.

This paper introduces a new frequency-reactive power (FQ) coefficient that shows the degree of dependence of the microgrid frequency on reactive power changes in each bus. The potential of controlling frequency through reactive power control can be used in islanded microgrids perfectly because

1) Most resources are connected to the grid through an inverter, which reduces inertia. Hence, the frequency drops faster.

2) The penetration level of renewable sources such as photovoltaic and wind turbines is high. These resources are exploited at the maximum power point and they cannot participate in frequency control through active power control.

3) The response rate of the resources that controls frequency through active power is low, such as fuel cells and micro-turbines.

4) Installation and maintenance costs of fast resources such as batteries are high.

5) Most resources are connected to the grid through an inverter, which facilitates the control of the reactive power by the inverter.

To the best knowledge of the authors, none of the research works (some of which mentioned above) have used reactive power management, which is called the channel of frequency-reactive power in this paper, to control frequency in microgrids. Indeed, all papers have used active power management like the active power generated by generators and storage devices for frequency control, which is the conventional channel of the frequency-active power for frequency control. This paper uses a new frequency control method to control the frequency of microgrids in an islanded mode. For this purpose, using the proposed coefficient, FQ, an optimum location is first indicated for the SOFC installation. Then, a coordinated reactive power management system is proposed between the SOFC and the battery. The proposed system is added to the conventional frequency control system. This proposed coordinated control system works similar to the secondary frequency control system, except that in this system the active power is transferred from the battery to other sources, but in the proposed system the reactive power is transferred from the battery to the SOFC. By doing this, the microgrid frequency drop is reduced and the frequency regulation becomes faster during contingencies. Also, the required storage capacity is significantly reduced and there would be no need to consider reserve capacity in the renewable sources for frequency control. Obviously, in any case, the voltage magnitude should remain in its acceptable standard range as suggested by the well-known curve of CBEMA (computer business equipment manufacturers association). In [29], the authors added an additional voltage control system to the conventional frequency control system to improve its performance in the islanded microgrid. The results were compared with the results of conventional control systems and their effectiveness was proven. The main focus was on the use of the potential of the battery and local control. But this paper proposes reactive power coordination between SOFC and the battery to improve the performance of the conventional frequency control system, and the results are compared with the results of the conventional frequency control system. This paper focuses on the coordination of the battery with SOFC to introduce this coordinated control system and present its advantages over the conventional control system. The paper does not concentrate on comparing this control system with the control system proposed in [29]. In their next research efforts, the authors will make a comprehensive technical and economic comparison between these two proposed methods.

The rest of the paper is organized as follows. Section 2 introduces a new frequency-reactive power (FQ) coefficient. Section 3 proposes a coordinated reactive power management system between the SOFC and the battery. Section 4 demonstrates the effectiveness of the proposed coefficient and coordinated system through various time domain simulations performed in the MATLAB/Simulink environment in a test microgrid. Finally, Section 5 presents the main contributions and conclusions of the paper.

## 2. PROPOSED FREQUENCY-REACTIVE POWER COEFFICIENT

A new coefficient that presents the effect of the reactive power variation of a bus on the microgrid frequency is defined in (1): "See (1)".

where $FQ_i$ is the frequency- reactive power coefficient of the *i*-th bus, $f_{MG}$ is the microgrid frequency, $P_{bat}$ is the total active load on the battery, $P_{load\ total}$ is the total active power load of the microgrid, $P_{load\ j}$ is the active load connected to the *j*-th bus, $|V_j|$ is the voltage magnitude of the *j*-th bus, $|V_k|$ is the voltage magnitude of the *k*-th bus (the battery is connected to the *k*-th bus), $Q_{bat}$ is the reactive power on the battery as a result of the reactive load variation connected to the *i*-th bus, and $Q_i$ is the reactive load connected to the *i*-th bus. In (1), the term $-(\sum_{j=1}^{n}[(\partial P_{load\ j}/\partial|V_j|)(\partial|V_j|/\partial|V_k|)(\partial|V_k|/\partial Q_{bat})(\partial Q_{bat}/\partial Q_i)])$ represents the total network load variations due to a change in the reactive power of the *i*-th bus ($\partial P_{load\ total}/\partial Q_i$). Factor $FQ_i$ indicates that if the reactive power in the *i*-th bus is changed to $\Delta Q_i$, the microgrid frequency is changed to $\Delta f_{MG}(\Delta f_{MG} = FQ_i \times \Delta Q_i)$.

This coefficient shows the degree of dependence of the microgrid frequency on the reactive power changes of the *i*-th bus. It is required that the coefficients $(\partial f_{MG}/\partial P_{bat})$, $(\partial P_{bat}/\partial P_{load\ total})_i$, $(\partial P_{load\ j}/\partial|V_j|)$, $(\partial|V_j|/\partial|V_k|)$, $(\partial|V_k|/\partial Q_{bat})$ and $(\partial Q_{bat}/\partial Q_i)$ be determined and substituted in (1) to obtain FQ for the *i*-th bus.

The VSI inverter typically interfaces between the storage devices (such as the battery) and the AC network. Using the energy stored in these devices, the VSI can have a behavior similar to the synchronous generator. Therefore, it can control the voltage magnitude and frequency in the isolated microgrid. In this case, the reference signals of the frequency and the voltage magnitude are calculated by the following equations [30]:

$$f_{MG} = f_{0\,MG} - (K_p \times P_{bat}) \quad (2)$$

$$|V_k| = |V_{0\,k}| - (K_q \times Q_{bat}) \quad (3)$$

where $f_{0\,MG}$ and $|V_{0\,k}|$ are the values of the microgrid frequency and the battery terminal voltage magnitude at the battery no-load conditions, respectively and $K_q$ and $K_p$ are the droop slopes of active power and reactive power, respectively. From (2) and (3), we have:

$$\partial f_{MG}/\partial P_{bat} = -K_P \quad (4)$$

$$\partial|V_k|/\partial Q_{bat} = -K_q \quad (5)$$

The exponential load model is used to illustrate the dependence of the active and reactive powers of the microgrid loads on the voltage magnitude [31]:

$$P_{load\ j} = P_{0j}(|V_j|/|V_{0\,j}|)^a \quad (6)$$

$$Q_{load\ j} = Q_{0j}(|V_j|/|V_{0\,j}|)^b \quad (7)$$

where $Q_{0j}$ and $P_{0j}$ are the reactive and active power consumptions of the *j*-th bus at voltage $V_{0j}$, respectively and *a* and *b* are the dependency coefficients of the active and reactive power of the load on the voltage magnitude, respectively. By rewriting (6) in terms of $|V_j|$, we have:

$$\partial P_{loadj}/\partial|V_j| = (a \times P_{0j}/|V_{0j}|) \times (|V_j|/|V_{0j}|)^{a-1} \quad (8)$$

The voltage magnitude of each bus in the system is affected by the changes in the voltages of other buses. The following equation shows changes in the voltage magnitude of the *j*-th bus due to changes in the *k*-th bus voltage magnitude [32]:

$$\Delta|V_j| = \Delta|V_k|(|Z_{jk}|/|Z_{kk}|) \quad (9)$$

where $|Z_{jk}|$ is the magnitude of the element of the *j*-th row and the *k*-th column of the impedance matrix, $|Z_{kk}|$is the element magnitude of the *k*-th row and the *k*-th column of the impedance matrix.

$(\partial Q_{bat}/\partial Q_i)$ is calculated by the following equation: "See (10)". $(\partial P_{bat}/\partial P_{load\ total})$ is calculated by the following equation: "see (11)".

where $K_{pf}$ is the coefficient of the dependence of the reactive power consumption on the frequency variations.

$$FQ_i = \partial f_{MG}/\partial Q_i = (\partial f_{MG}/\partial P_{bat}) \times (\partial P_{bat}/\partial P_{load\ total})_i \times \sum_{j=1}^{n}[(\partial P_{load\ j}/\partial|V_j|)(\partial|V_j|/\partial|V_k|)(\partial|V_k|/\partial Q_{bat})(\partial Q_{bat}/\partial Q_i)] \quad (1)$$

$$\frac{\partial Q_{bat}}{\partial Q_i} = \frac{1}{\left[\left(\frac{b \times Q_{0i}}{|V_{0i}|^b}\right)\left(\frac{-K_q \times |Z_{ik}|}{|Z_{kk}|}\right)\left[V_{0i} + \left(\frac{|Z_{ik}|}{|Z_{kk}|}\right)(-K_q \times Q_{Bat})\right]^{b-1}\right]} \quad (10)$$

$$\frac{\partial P_{bat}}{\partial P_{load\ total}} = \frac{1}{[(-K_{pf} \times K_p)\sum_{j=1}^{n}[(P_{0\ j})\left(\frac{|V_{0\,j}| + (|Z_{jk}|/|Z_{kk}|)(-K_q \times Q_{Bat})}{|V_{0j}|}\right)^a]} \quad (11)$$

An equation for calculating FQ of each bus can be obtained by replacing equations (4), (5), (8), (9), (10) and (11) in (1).

## 3. COORDINATION CONTROL OF REACTIVE POWER THE SOFC AND THE BATTERY

In the normal mode, a microgrid is always connected to the upstream network. In this case, the microgrid voltage magnitude and the frequency are determined by the upstream network as an infinite bus. There is a balance between the active and reactive power generation and consumption in the microgrid and any imbalance is compensated by the upstream network. Following a fault in the upstream network or a maintenance program, in theemergency mode, the microgrid can separate from the upstream grid and operate independently. At the moment of disconnection, there is a need for energy storage such as a battery to play the role of the upstream network and to compensate for the imbalance in the production and consumption of the microgrid power in the shortest possible time. In this case, the battery determines the frequency and voltage magnitude of the microgrid with respect to its active and reactive power from (2) and (3), respectively.

At the moment of disconnection, it is possible to change the voltage magnitude in its acceptable standard range (such as the well-known curve of CBEMA) by managing the reactive power of the battery. The well-known curve of the affiliated computer business equipment manufacturers association (CBEMA) that is shown in Fig. 1 can be applied to assess the voltage quality in the case of the voltage drop/rise. The CBEMA curve shows the magnitude and duration of voltage variations in the power system [33]. As such, the total active power consumption of the microgrid and the resulting active power on the battery will change. Therefore, at the critical moment of disconnection, the frequency of the microgrid can be controlled more effectively.

The SOFC reactive power control can be used to control the reactive power of the battery. In the microgrid, the SOFC is connected to the grid via power electronics interfaces. Inverter control strategies are generally divided into two types:

**1) PQ Inverter Control:** the inverter is used to provide a specific active and reactive power.

**2) Voltage source inverter control:** the inverter is controlled to supply the load with the predetermined voltage magnitude and frequency.

The SOFC inverter is in the PQ control mode, and it can be used to control the reactive power generation or consumption of the SOFC easily and quickly.

According to (2), the reactive power of the battery to generate the voltage magnitude corresponding to the CBEMA curve is calculated by the following equation:

$$Q_{CBEMA} = (|V_0| - |V_{CBEMA}|)/K_q \quad (12)$$

where $|V_{CBEMA}|$ is the voltage magnitude corresponding to the CBEMA curve and $Q_{CBEMA}$ is the reactive power of the battery to create $|V_{CBEMA}|$. The required reactive power of the SOFC to generate reactive power $Q_{CBEMA}$on the battery is calculated by

$$Q_{SOFC} = Q_{battery} - Q_{0\,SOFC} - Q_{CBEMA} \quad (13)$$

where $Q_{SOFC}$ is the reactive power of the SOFC, $Q_{battery}$ is the reactive power of the battery, and $Q_{0\,SOFC}$ is the reactive power of the SOFC before being disconnected from the upstream network. By replacing equation (12) in (13), we have:

$$Q_{SOFC} = Q_{battery} - Q_{0\,SOFC} - ((|V_0| - |V_{CBEMA}|)/K_q) \quad (14)$$

Therefore, a supplementary reactive power controller can be added to the SOFC control system according to Fig. 2. The aim of this controller is to coordinate the reactive power of the SOFC and the battery to better control the frequency of the microgrid.

By stopping the frequency changes, after a short time and as soon as the frequency is stabilized, the battery load must be removed and supplied by controllable generation sources such as fuel cells and micro turbines. The secondary frequency control system shown in Fig. 3 does just that. The micro source active power (MS) to return the frequency to the nominal value is determined.

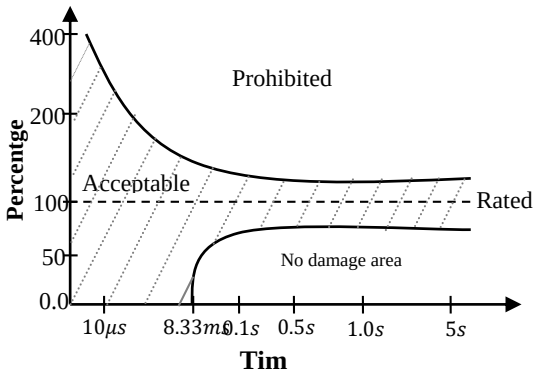


**Fig. 1:** The CBEMA curve.

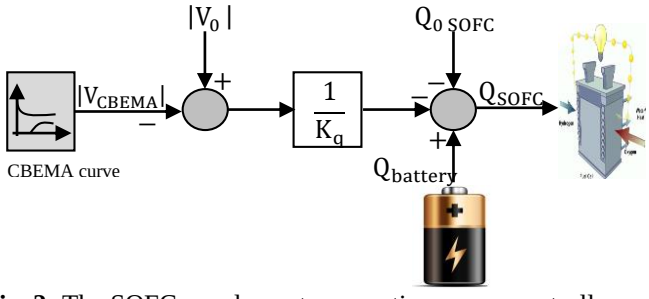


**Fig. 2:** The SOFC supplementary reactive power controller.

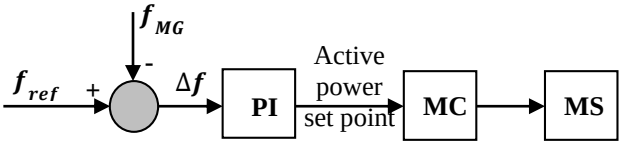


**Fig. 3:** The secondary frequency control system.

## 4. SIMULATION RESULTS

### 4.1. Test System

This paper uses a test system, as shown in Fig. 4, to demonstrate the effectiveness of the new coefficient and the proposed coordinated reactive power controller. This system is a low-voltage 400 V microgrid, which is simulated in the MATLAB/Simulink environment. This system is connected to an upstream medium-voltage network. The microgrid operates in normal conditions and in case of a fault in the upstream network, just after the fault, the microgrid is disconnected from the upstream network and operates independently. In this microgrid, the nominal ratings of the SOFC, the PV array, and the battery are 100kW, 10 kW, and 50 kW, respectively. The total load of the microgrid is 50 kVA, which is of constant impedance type and is distributed on buses 9 to 13. The details of active and reactive consumption of each bus are presented in Table 1. The capacitance of the lines is ignored due to their short length, and only the resistance and inductance of the lines are modeled. The length and impedance of the test microgrid lines are presented in Table 2.

### 4.2. The Results of The Frequency-Reactive Power Coefficient

For the test microgrid, the coefficient $(\partial Q_{bat}/\partial Q_i)$ of (10) and the coefficient $(\partial P_{bat}/\partial P_{load\ total})$ of (11) is calculated for all buses. The results are presented in Tables 3 and 4, respectively. Then, using (1), the coefficient FQ is calculated for all microgrid buses. The results are presented in Table 5. The parameters used to calculate these coefficients are given in Table 6. It is possible to rank the microgrid buses based on the values of this coefficient in terms of the effectiveness of reactive power injections on the frequency of the grid. This is performed for the test microgrid and the results are presented in Table 7. From the values of this table, it is concluded that buses 2 and 3 are the first priorities and buses 4 and 12 are the last priorities in the installation of reactive power control devices for frequency control. Therefore, in the test microgrid, the SOFC is installed in bus 2.

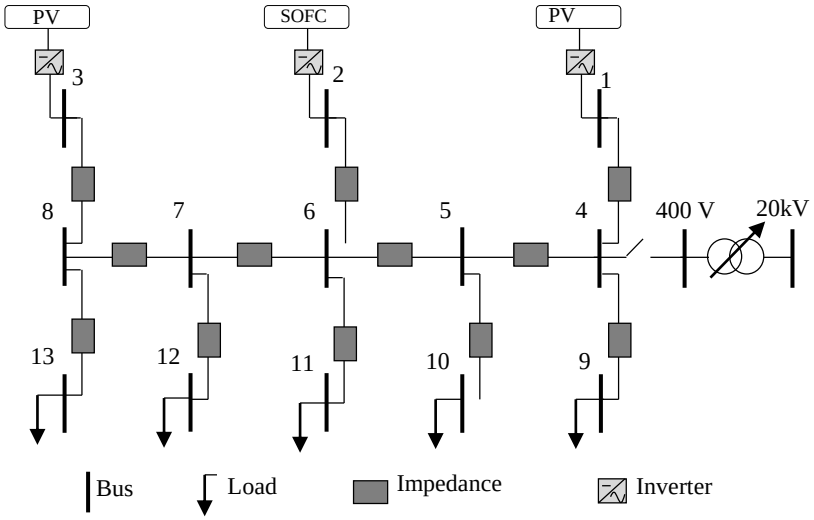


**Fig. 4:** The test low-voltage microgrid.

**Table 1:** The active ($P_{Load}$) and reactive ($Q_{Load}$) load of the *i*-th bus.

| i | $P_{load}$(kW) | $Q_{load}$(kVar) |
|---|---|---|
| 9 | 10 | 4 |
| 10 | 15 | 6 |
| 11 | 15 | 6 |
| 12 | 10 | 5 |
| 13 | 10 | 4 |

**Table 2:** The line length ($L_{nm}$) and impedance ($Z_{nm}$)

| n | m | $L_{nm}$(M) | $Z_{nm}$(Ω) |
|---|---|---|---|
| 4 | 1 | 30 | 0.024 + j0.0023 |
| 4 | 9 | 30 | 0.024 + j0.0023 |
| 4 | 5 | 100 | 0.028+ j0.0083 |
| 5 | 10 | 30 | 0.024 + j0.0023 |
| 5 | 6 | 100 | 0.028+ j0.0083 |
| 6 | 2 | 30 | 0.024 + j0.0023 |
| 6 | 11 | 30 | 0.024 + j0.0023 |
| 6 | 7 | 100 | 0.028+ j0.0083 |
| 7 | 12 | 30 | 0.024 + j0.0023 |
| 7 | 8 | 100 | 0.028+ j0.0083 |
| 8 | 3 | 30 | 0.024 + j0.0023 |
| 8 | 13 | 30 | 0.024 + j0.0023 |

**Table 3:** The values of $(\partial Q_{bat}/\partial Q_i)$ for all buses.

| Bus number(i) | $\partial Q_{bat}/\partial Q_i$ |
|---|---|
| 1 | 0.8768 |
| 2 | 0.8769 |
| 3 | 0.8814 |
| 4 | 0.8758 |
| 5 | 0.8781 |
| 6 | 0.8755 |
| 7 | 0.8770 |
| 8 | 0.8810 |
| 9 | 0.8784 |
| 10 | 0.8761 |
| 11 | 0.8773 |
| 12 | 0.8777 |
| 13 | 0.879 |

**Table 4:** The values $(\partial P_{bat}/\partial P_{load\ total})$ for all buses.

| Bus number(i) | $(\partial P_{bat}/\partial P_{load\ total})_i$ |
|---|---|
| 1 | 0.9411 |
| 2 | 0.7397 |
| 3 | 0.8041 |
| 4 | 0.9820 |
| 5 | 0.8483 |
| 6 | 1.1978 |
| 7 | 0.8632 |
| 8 | 0.9256 |
| 9 | 0.8832 |
| 10 | 0.7062 |
| 11 | 1.2161 |
| 12 | 0.8366 |
| 13 | 0.8674 |

**Table 5:** The values of coefficient FQ for all buses.

| Bus number | FQ (Hz/MVar) |
|---|---|
| 1 | 5.4831 |
| 2 | 5.2890 |
| 3 | 7.727 |
| 4 | 4.459 |
| 5 | 5.591 |
| 6 | 5.842 |
| 7 | 5.457 |
| 8 | 7.607 |
| 9 | 5.372 |
| 10 | 6.202 |
| 11 | 5.085 |
| 12 | 4.680 |
| 13 | 5.963 |

**Table 6:** The parameters of the test system in calculating FQ.

| |
|---|
| $K_p = 1.2566 \times 10^{-4}\ \mathrm{Rad}/(\mathrm{s.W})$ |
| $K_q = 3 \times 10^{-6}\ \mathrm{p.u/Var}$ |
| $Q_{0\,SOFC} = 0$ |
| a=2 |
| b=2 |
| $K_{pf} = 1.8$ |
| $\lvert V_k \rvert = 1\ \mathrm{p.u}$ |

**Table 7:** The FQ values from the highest to the lowest.

| Bus number | FQ (Hz/MVar) |
|---|---|
| 3 | 7.7277 |
| 2 | 7.6079 |
| 10 | 6.2026 |
| 13 | 5.9639 |
| 6 | 5.8423 |
| 5 | 5.5913 |
| 1 | 5.4831 |
| 7 | 5.4578 |
| 9 | 5.3722 |
| 8 | 5.2890 |
| 11 | 5.0859 |
| 12 | 4.6807 |
| 4 | 4.4590 |

### 4.3. Results of the Coordinated Control of Reactive Power

It is assumed that the test microgrid is connected to the upstream network and at time t = 10 s, suddenly a fault occurs and the microgrid is disconnected and operates independently. In this case, three different scenarios are considered and compared:

**Scenario 1**: The microgrid voltage magnitude is constant and its frequency is controlled according to (1).

**Scenario 2**: The microgrid frequency is controlled according to (1), and its voltage magnitude is controlled according to (2) (the conventional frequency control system).

**Scenario 3**: In the conventional frequency control system, coordinated reactive power management between the SOFC and the battery is established for the better control of the frequency (the proposed frequency control system).

The microgrid frequency is shown in Fig. 5 for various scenarios. It is clear that the use of scenario 3 leads to a small decrease in the frequency of the network following the disconnection from the upstream network and it prevents the frequency to be out of permissible range at the initial moments and provides more time for the secondary frequency controller to return the frequency to the nominal value. It is also seen that scenario 2 outperforms scenario 1. This shows that the voltage participation in the control of the frequency is appropriate and effective.

The voltage magnitude of different buses of the microgrid under scenario 3 is shown in Fig. 6. It can be seen

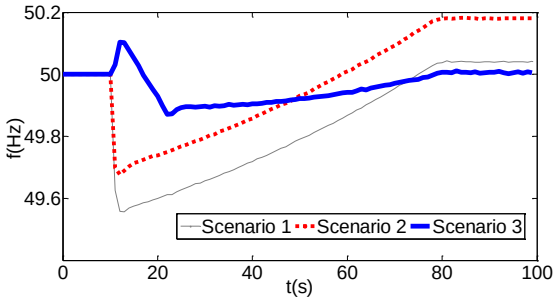


**Fig. 5:** Microgrid frequency under various scenarios.

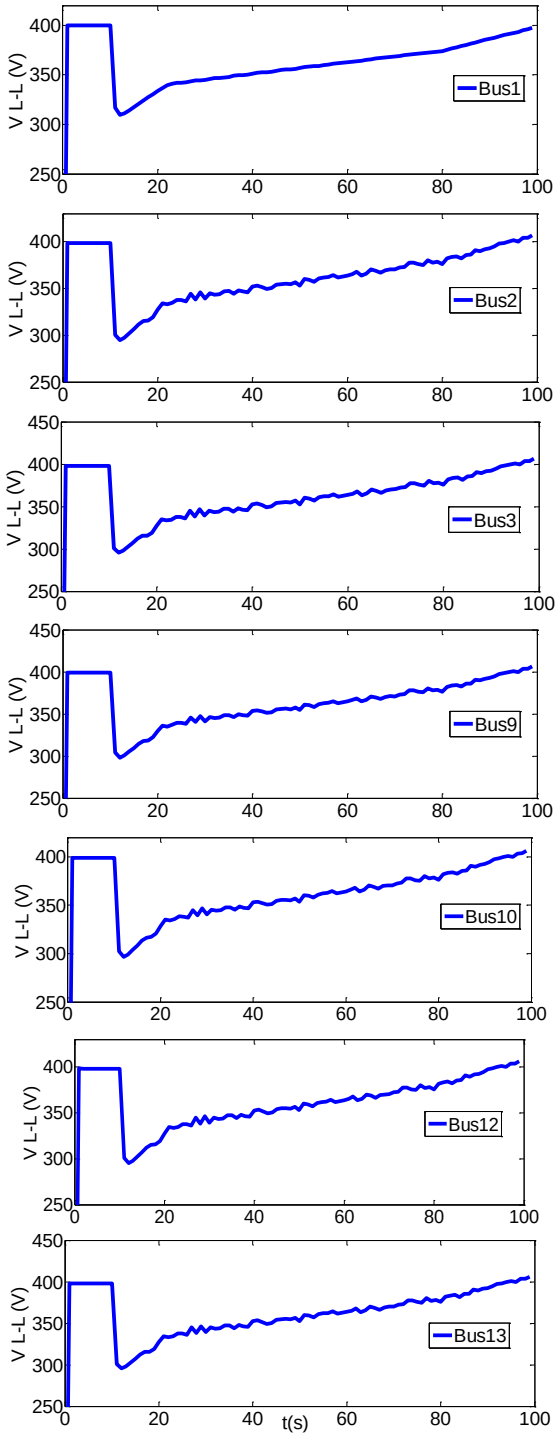


**Fig. 6:** Voltage magnitude of different buses under scenario 3.

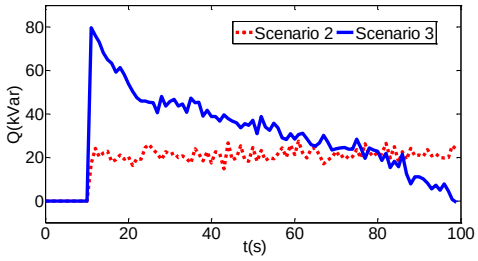


**Fig. 7:** The battery reactive power under various scenarios.

that the voltage magnitude of all buses, even the remote end buses, follows the CBEMA requirements. The drop in the voltage magnitude created for the specified periods of time is acceptable according to the CBEMA curve. After a short time and as soon as the frequency is stabilized, as the frequency goes toward the nominal value, the voltage tends to the nominal voltage and it returns to the nominal voltage as soon as the frequency returns to the nominal value. The voltage magnitudes of all buses are almost the same due to the small size of the microgrid.

The reactive power of the battery under scenarios 2 and 3 is shown in Fig. 7. It can be seen that in scenario 2, the reactive power of the battery is almost constant and does not participate in frequency control. While in scenario 3, it is controlled by SOFC and coordinated reactive power management. In the steady state after the fault, the reactive power of the battery is zero, and the reactive power required by the SOFC is provided.

The reactive power of the SOFC under scenarios 2 and 3 is shown in Fig. 8. The reactive power of the SOFC is assumed to be zero before disconnection. Also, in the conventional frequency control system, the SOFC does not participate in frequency control. So, as shown in Fig. 8, the reactive power of the SOFC in scenario 2 is always zero. However, in Scenario 3, the reactive power of the SOFC is not zero to participate in frequency control and it is adjusted by the coordinated control system. In the steady state after the fault, the SOFC provides all the required reactive power of the microgrid. The reactive power of the PV is assumed to be zero before and after the fault, and the PV does not participate in the reactive power control of the microgrid.

Fig. 9 presents the battery's active power in various scenarios. In this figure, it can be seen that the active power of the battery in scenario 3 is less than that of the other scenarios. As a result, a lower capacity battery can be used in Scenario 3, and the cost of energy storage will be reduced. It is also seen that in all scenarios, with the function of the secondary frequency control system, after a period of time, the active load is transferred from the wind to the battery and the active power of the battery becomes zero. It is also seen that in all scenarios after a period of time, with the function of the secondary frequency control system, the active load is transferred from the battery to the SOFC and the active power of the battery becomes zero. Scenario 3 also performs better in this situation.

Fig. 10 depicts the SOFC active power in various scenarios. It can be seen that the SOFC active power is almost the same in all three scenarios and, after the operation of the secondary frequency control system, it rises from the initial value of 25 kW to 50 kW in the steady state.

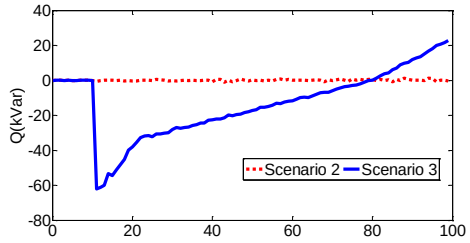


**Fig. 8:** The SOFC reactive power under various scenarios.

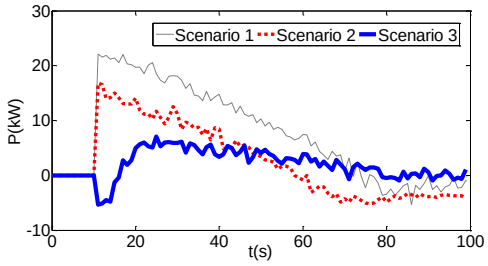


**Fig. 9:** The battery active power under various scenarios.

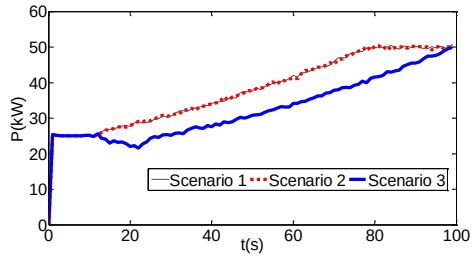


**Fig. 10:** The SOFC active power under various scenarios

All the entire imbalance in the active power generation and consumption is compensated by the SOFC.

The power of the PV under various scenarios is shown in Fig. 11 according to which in all three scenarios, before and after the fault, the PV active power is constant and is equal to its maximum value (10 kW). In this case, the maximum PV capacity is used, and no storage capacity is considered for frequency control.

The voltage magnitude corresponding to the CBEMA curve ($|V_{CBEMA}|$) is shown in Fig. 12. According to the curve of the CBEMA, severe voltage drop (even near zero) is allowed for a very short time.

## 5. Conclusion

This paper proposed the idea of using reactive power to control the frequency in the islanded microgrid. To indicate the amount of change in the frequency due to changes in reactive power in each bus, the frequency-reactive power coefficient (FQ) was introduced. The microgrid buses can be prioritized based on the values of this coefficient, and the appropriate location to install SOFC can be determined. The proposed coefficient is new and has not been presented in any other reference. With this coefficient, the buses can be found in which the change in their reactive power will have the greatest effect on the change in the microgrid frequency. The reactive power control sources can be installed in those buses for this purpose. Also, this paper proposed the coordinated

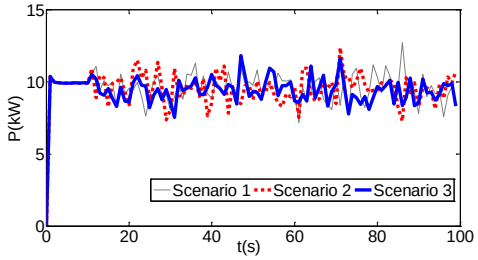


**Fig. 11:** The PV active power under various scenarios.

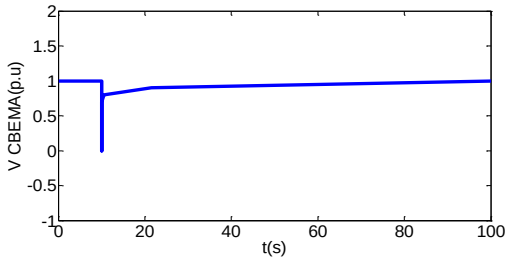


**Fig. 12:** The voltage magnitude corresponding to the CBEMA curve ( $|V_{CBEMA}|$).

controller and the new coefficient were proven by the simulations performed in MATLAB/Simulink environment. The simulation results showed that the proposed coordinated control system outperformed the conventional frequency control system. This coordinated controller has many advantages such as reducing frequency drop at the moment of disconnection, faster frequency settling time to its nominal value, reducing the required battery capacity and the ability to operate renewable resources in maximum power point. These advantages presented and interpreted in detail in the Results section improve system stability and equipment performance and reduce costs due to more efficient use of renewable resources and the need for smaller batteries.

## CRediT Authorship Contribution Statement

**Saeed Aminzadeh:** Conceptualization, Data curation, Formal analysis**,** Funding acquisition**,** Methodology, Project administration**,** Resources, Software**,** Visualization, Roles/Writing - original draft**,** Writing - review & editing. **Mehrdad Tarafdar Hagh:** Investigation, Supervision, Validation. **Heresh Seyedi**: Investigation, Supervision, Validation.

## Declaration of Competing Interest

The authors declare that they have no known competing financial interests or personal relationships that could have appeared to influence the work reported in this paper. The ethical issues; including plagiarism, informed consent, misconduct, data fabrication and/or falsification, double publication and/or submission, redundancy has been completely observed by the authors.

## References

[1] J. Lai, X. Lu, and X. Yu, "stochastic distributed frequency and load sharing control for microgrids with communication delays," *IEEE Systems Journal*, vol. 13, no. 4, pp. 4269 - 4280, 2019.

[2] C. Wang, S. Mei, Q. Dong, and R. Chen, "Coordinated Load Shedding Control Scheme for Recovering

Frequency in Islanded Microgrids," *IEEE Access*, vol. 8, no. 1, pp. 215388 – 215398, 2020.

[3] G. Delille, B. Francois, and G. Malarange, "Dynamic frequency control support by energy storage to reduce the impact of wind and solar generation on isolated power system's inertia," *IEEE Trans. Sustain. Energy*, vol. 3, no. 4, pp. 931–939, 2012.

[4] K. W. Joung, T. Kim, and J. W. Park, "Decoupled Frequency and Voltage Control for Stand-Alone Microgrid with High Renewable Penetration," *IEEE Transactions on Industry Applications*, vol. 55, no. 1, pp. 122 - 133, 2019.

[5] H. Zhao, M. Hong, W. Lin, and K. A. Loparo, "Voltage and Frequency Regulation of Microgrid with Battery Energy Storage Systems," *IEEE Transactions on Smart Grid*, vol. 10, no. 1, pp. 414 - 424, 2019.

[6] J. Li, R. Xiong, Q. Yang, F. Liang, and W. Yuan, "Design/test of a hybrid energy storage system for primary frequency control using a dynamic droop method in an isolated microgrid power system," *Applied Energy*, vol. 201, 1 September, pp. 257-269, 2017.

[7] S. Acharya, M. S. El Moursi, and A. Al-Hinai, "Coordinated Frequency Control Strategy for an Islanded Microgrid with Demand Side Management Capability," *IEEE Transactions on Energy Conversion*, vol. 33, no. 2, pp. 639 - 651, 2018.

[8] E. Karfopoulos, L. Tena, A. Torres, P. Salas, and N. Hatziargyriou, "A multi-agent system providing demand response services from residential consumers," *Electric Power Systems Research*, vol. 120, March, pp. 163-176, 2015.

[9] E. S. N. Raju, and P. Trapti Jain, "Impact of load dynamics and load sharing among distributed generations on stability and dynamic performance of islanded AC microgrids," *Electric Power Systems Research*, vol. 157, April, pp. 200-210, 2018.

[10] C. Gouveia, J. Moreira, C. L. Moreira, and J. A. Peças Lopes, "Coordinating Storage and Demand Response for Microgrid Emergency Operation," *IEEE Trans. Smart Grid*, vol. 4, no. 4, pp. 1898 – 1908, 2013.

[11] P. Jampeethong and S. Khomfoi, "Coordinated Control of Electric Vehicles and Renewable Energy Sources for Frequency Regulation in Microgrids," *IEEE Access*, vol. 8, no. 1, pp. 141967 - 141976, July 2020.

[12] A. Molina-Garcia, F. Bouffard, and D. Kirschen, "Decentralized demand-side contribution to primary frequency control," *IEEE Trans. Power Syst*, vol. 26, no. 1, pp. 411–419, Feb. 2011.

[13] M. Marzband, M. M. Moghaddam, M. F. Akorede, and G Khomeyrani, "Adaptive load shedding scheme for frequency stability enhancement in microgrids," *Electric Power Systems Research*, vol.140, November, pp. 78-86, 2016.

[14] M. Farrokhabadi, C. A. Cañizares, and K. Bhattacharya, "Frequency Control in Isolated/Islanded Microgrids Through Voltage Regulation," *IEEE Trans. Smart Grid*, vol. 8, no. 3, pp. 1185 – 1193, 2017.

[15] E. Rokrok, M. Shafie-khah, and J. P. S. Catalão, "Review of primary voltage and frequency control methods for inverter-based islanded microgrids with distributed generation," *Renewable and Sustainable Energy Reviews*, vol. 82, Part 3, pp. 3225-3235, February. 2018.

[16] N. Cai and J. Mitra, "A multi-level control architecture for master-slave organized microgrids with power electronic interfaces," *Electric Power Systems Research*, vol.109, April, pp. 8-19, 2014.

[17] K. Sh, H. Ye, W. Song, and N. Zhou, "Virtual Inertia Control Strategy in Microgrid Based on Virtual Synchronous Generator Technology," *IEEE Access*, vol. 6, May, pp. 27949 – 27957, 2018.

[18] J. Liu, M. J. Hossain, J. Lu, F. H. M. Rafi, and H. Li, "A hybrid AC/DC microgrid control system based on a virtual synchronous generator for smooth transient performances," *Electric Power Systems Research*, vol. 162, September, pp. 169-182, 2018.

[19] N. Sockeel, J. Gafford, B. Papari, and M. Mazzola, "Virtual Inertia Emulator-Based Model Predictive Control for Grid Frequency Regulation Considering High Penetration of Inverter-Based Energy Storage System," IEEE *Transactions on Sustainable Energy* , vol. 11, no.4, pp. 27949 – 27957, 2020.

[20] O. Babayomi, Z. Li, and Z. Zhang, "Distributed secondary frequency and voltage control of parallel-connected vscs in microgrids: A predictive VSG-based solution," *CPSS Transactions on Power Electronics and Applications*, vol. 5,no. 4, pp. 342 - 351, 2020.

[21] X. Wu, C. Shen, and R. Iravani, "A Distributed, Cooperative Frequency and Voltage Control for Microgrids," *IEEE Trans. Smart Grid*, vol. 9, no. 4, pp. 2764 – 2776, 2018.

[22] R. Jalilzadeh Hamidi, H. Livani, S. H. Hosseinian and, G. B. Gharehpetian, "Distributed cooperative control system for smart microgrids," *Electric Power Systems Research*, vol. 130, January, pp. 241-250, 2016.

[23] T. John and S. P. Lam, "Voltage and frequency control during microgrid islanding in a multi-area multi-microgrid system," *IET Generation, Transmission & Distribution*, vol.11, no. 6, pp. 1502 – 1512, May 2017.

[24] A. Nisar and M. S. Thomas, "Comprehensive Control for Microgrid Autonomous Operation with Demand Response," *IEEE Trans. Smart Grid*, vol. 12, no. 99, pp.1 – 9, 2016.

[25] M.H. Khooban, "Secondary Load Frequency Control of Time-Delay Stand-Alone Microgrids With Electric Vehicles," IEEE Trans. Industrial Electronics, vol. 65, no. 9, pp. 7416 – 7422, Sept. 2018.

[26] A. Jeya Veronica and N. Senthil Kumar, "Internal Model Based Load Frequency Controller Design for Hybrid Microgrid System," Energy Procedia, vol. 117, June, pp. 1032-1039, 2017.

[27] M. Kosar and S. Hossein, "Decentralized Reactive Power Sharing and Frequency Restoration in Islanded Microgrid," IEEE Trans. Power Systems, vol. 32, no. 4, pp. 2901 – 2912, July 2017.

[28] Y.S. Kim, E. S. Kim, and S. Moon, "Distributed Generation Control Method for Active Power Sharing and Self-Frequency Recovery in an Islanded Microgrid," IEEE Trans. Power Systems, vol. 32, no. 1, pp. 544 – 551, 2017.

[29] S. Aminzadeh, M. Tarafdar Hagh, and H. Seyedi, " Reactive power management for microgrid frequency control," *International Journal of Electrical Power & Energy Systems*, Vol. 120, pp. 105959, 2020.

[30] J. Moreira, C. L. Moreira, and J. A. Peças Lopes, "Defining control strategies for microgrids islanded operation," *IEEE Trans Power Syst*,Vol. 21, no. 2, pp. 916-924, 2006.

[31] P. Kundur, *Power System Stability and Control*. New York, McGraw- Hill, 1994.

[32] H. Saadat, *Power System Analysis*. New Delhi, Tata McGraw-Hill, 2002.

[33] J. Arrillaga, N. R. Watson, and Shipu Che, *Power System Quality Assessment*. John Wiley & Sons, 2000.

## BIOGRAPHY

**Saeed Aminazadeh** received his B.Sc. degree in electrical engineering at Shahid Beheshti University, Tehran, Iran in 2008, M.Sc. degree in electric power engineering at the Shahid Chamran University of Ahvaz, Ahvaz, Iran in 2010, and his Ph.D. degree in power engineering at the University of Tabriz, Tabriz, Iran in 2020. He has been with the Faculty of Engineering, Islamic Azad University since 2011. His current research interests include modeling, control, and optimization in microgrids.

**Mehrdad Tarafdar Hagh** received his B.Sc., M.Sc. (Hons.), and Ph.D. degrees in power engineering at the University of Tabriz, Tabriz, Iran in 1989, 1992, and 2000, respectively. He has been with the Faculty of Electrical and Computer Engineering, the University of Tabriz since 2000 where he is currently a professor. He has published more than 200 papers in power systems and power-electronic-related topics. His interest topics include power system operation, distributed generation, flexible ac transmission systems, and power quality.

**Heresh Seyedi** was born in Iran in 1979. He received his B.Sc., M.Sc., and Ph.D. degrees in electrical engineering at the University of Tehran, Tehran, Iran, in 2001, 2003, and 2008, respectively. Currently, he is with the faculty of Electrical and Computer Engineering, University of Tabriz, Tabriz, Iran. His areas of interest include digital protection of power systems and power system transients.